Materials Letters 209 (2017) 111–114

Contents lists available at ScienceDirect

Materials Letters

journal homepage: www.elsevier.com/locate/mlblue

Solid-state synthesis of pure and doped lanthanide oxide nanomaterials by using polymer templates. Study of their luminescent properties

C. Diaz [a,*], M.L. Valenzuela [b], C. García [a], R. de la Campa [c], A. Presa Soto [c,*]

[a] Departamento de Química, Facultad de Química, Universidad de Chile, La Palmeras 3425, Nuñoa, casilla 653, Santiago de Chile, Chile
[b] Universidad Autónoma de Chile, Instituto de Ciencias Químicas Aplicadas, Inorganic Chemistry and Molecular Material Center, Av. El Llano Subercaseaux 2801, San Miguel, Santiago de Chile, Chile
[c] Departamento de Química Orgánica e Inorgánica (IUQOEM), Facultad de Química, Universidad de Oviedo, Julián Clavería s/n, 33006 Oviedo, Spain

ARTICLE INFO

Article history:
Received 21 March 2017
Received in revised form 5 July 2017
Accepted 26 July 2017
Available online 27 July 2017

Keywords:
Polymer-templated
Lanthanide oxide
Chitosan
Europium-doped

ABSTRACT

We herein reports the solid-state synthesis of pure and doped lanthanide oxides by using polymeric materials (chitosan and polystyrene-*co*-poly(4-vinylpyridine), PS-co-P4VP) as a solid template. Lanthanide nanomaterials are prepared in two-step methodology combining both solution and solid procedures. The first involves the synthesis of macromolecular complexes Chitosan·[$M(NO_3)_3$//$M'(NO_3)_3$] and PS-*co*-P4VP·[$M(NO_3)_3$//$M'(NO_3)_3$] (M = La, Pr; M′ = Eu); and the second consists in the pyrolysis at 800 °C of the as-prepared solid macromolecular complexes. The pyrolytic products were characterized by X-ray diffraction, SEM-EDS, TEM, and HR-TEM. Whereas similar particle size distribution in average (*ca.* 25 nm) was observed with both polymer templates, a higher degree of crystallinity was obtained by using PS-*co*-P4VP. Importantly, the emission luminescent intensity of the doped pyrolytic oxides, La_2O_3//Eu_2O_3 and $PrO_{1,83}$//Eu_2O_3, is not quenched despite the presence of dopant. Thus, the as-prepared doped oxides exhibit an enhanced Eu^{3+} emission originated from the $^5D_0 \rightarrow {}^7F_n$ (n = 1, 2, 3, 4) transitions, which is more intense for the PS-*co*-P4VP template. This synthetic methodology base on the pyrolysis of polymeric complexes can be considered as a general and straightforward methodology leading to pure and Eu^{3+}-doped nanostructured lanthanide oxide.

1. Introduction

Nanostructured metal oxides materials have attracted enormous scientific and technological interest in multidisciplinary research field [1]. In this regard, lanthanide oxides have received special attention due to their unique optical and magnetic properties arising from the electron configurations of the 4*f* orbitals [2,3]. For most of practical applications like in laser amplifiers, a high crystallinity of these lanthanide materials is required, which often needs of their inclusion into a solid matrices [2–5]. This inclusion is often problematic when the lanthanide material was prepared from solution synthetic methodologies which require additional synthetic steps including the evaporation of the generated solution of nanoparticles and the subsequent formation of super lattices [6–8]. Thus, the development of new methods to produce nanoparticles directly in solid-state is of pivotal importance [9]. The main synthetic pathways to lanthanide oxides are the precipitation/co-precipitation route, the sol-gel route, the Hydrothermal/Solvothermal route, and the thermal decomposition route, among others [2,5]. Although some very specific solid state thermal preparation methods have been reported [9,10], to date, there is a lack of general routes to nanostructured rare earth metal oxides [10]. On the other hand, the most usual synthetic route to doped lanthanide materials is the co-precipitation method [11–13]. Thus, we herein report a general method to prepare lanthanide metal oxides, pure and doped. This method is based on the solid-state pyrolysis of the macromolecular complexes of general formula (polymer)·[$M(NO_3)_3$//$M'(NO_3)_3$] (polymer = Chitosan or PS-*co*-P4VP; M′ = Eu^{3+}; and M = lanthanide. See Scheme S1 in the Supp. Info.).

2. Material and methods

2.1. Synthesis of pure and Eu^{+3}-doped nanostructured lanthanide materials

The macromolecular complexes Chitosan·[$M(NO_3)_3$//$M'(NO_3)_3$] and PS-*co*-P4VP·[$M(NO_3)_3$//$M'(NO_3)_3$] (M = La, Pr; M′ = Eu;

* Corresponding authors.
E-mail addresses: cdiaz@uchile.cl (C. Diaz), presaalejandro@uniovi.es (A. Presa Soto).

http://dx.doi.org/10.1016/j.matlet.2017.07.112
0167-577X/

PS-*co*-P4VP = poly(4-vinylpyridine)-*co*-polystyrene) were prepared according to a previous synthetic methodology described by us [14,15]. In a typical synthesis, the lanthanide salts and the polymers (chitosan or PS-*co*-P4VP) are placed into a Schlenk tube with CH_2Cl_2, and the mixture was stirred for 10 days. Then, the solvent was removed under vacuum and the macromolecular complexes are obtained as solids in very high yields (*ca.* 90%).

In a second step, the solid macromolecular complexes, Chitosan·[$M(NO_3)_3$//$M'(NO_3)_3$] and PS-*co*-P4VP[$M(NO_3)_3$//$M'(NO_3)_3$], were pyrolized at 800 °C under air atmosphere by using a temperature ramp (heating rate = 10 °C/min, time = 5 h, furnace Wisd WiseTherm FHP-12, Daihan Scientific, Co. Ltd). The pyrolyzed samples were characterized by SEM (JSM-6380LV, Jeol Ltd. Microscope), HR-TEM (JEOL 2011, Ltd. Microscope. XRD using a Siemens D-5000 diffractometer with a Cu-Kα radiation of (40 kV, 30 mA)), and a graphite monochromator (λ = 1.540598 Å). Fluorescence spectroscopy was performed using a Jasco FP-8200 fluorimeter with a solid-state accessory. ICP-mass analysis were performed in a Perkin-Elmer Elan 9000 (detection limit 0.0003%).

3. Results and discussion

Both polymeric templates, chitosan (having $-NH_2$ and –OH groups in the repeat unit), and PS-*co*-P4VP (having randomly distributed pyridine groups along the chains), ensure the homogeneous distribution of metal salts along the polymeric chains. The structure of the pyrolytic products (pure and doped) was confirmed by X-ray diffractions (XRD) patterns (Fig. 1 and S1 in Sup. Info.). The XRD patterns of the as-prepared pure La_2O_3 and $PrO_{1.83}$ from both PS-*co*-P4VP and chitosan, were consistent with the presence of the standard structures of the BCC and FCC lattices of the La_2O_3 and $PrO_{1.83}$ respectively. However, according to the broadness of the peaks obtained from both polymeric templates, it is clear that more crystalline phases were obtained from PS-*co*-P4VP.

Similar behavior was observed from the XRD patterns of the as-prepared doped La_2O_3 and $PrO_{1.83}$ (Fig. S1 in Sup. Info.). Whilst more crystalline phases were also achieved from PS-*co*-P4VP, we observed that the XRD reflections of the doped oxides were slightly shifted to lower angles (2θ) compared to reflections of pure oxides due to the incorporation of larger Eu^{+3} ions into the lattices of La_2O_3 and $PrO_{1.83}$.

SEM images of pure (Fig. 2) and Eu^{+3}-doped La_2O_3 and $PrO_{1,83}$ materials (Fig. S2 in Supp. Info.), showed a very similar porous structure for all the as-prepared oxides independently of the solid polymeric templated used in their preparation. The EDX spectrum of pure and doped La_2O_3 and $PrO_{1,83}$ materials (Fig. 2 and S2 in Sup. Info), showed no elements other than La, Pr and O for pure materials, and also Eu in doped oxides, which supports the purity of the as-prepared materials.

HR-TEM and the SAED patterns of the pure and doped $PrO_{1,83}$ prepared from both Chitosan and PS-*co*-4-PVP are showed in Fig. 3 and S3 in the Sup. Info. The calculated interference fringe spacing of both pure and doped $PrO_{1,83}$ materials was approximately 0.32 nm, being consistent with the interplanar distance of the (1 1 1) plane in the face-centered cubic structure of $PrO_{1,83}$ [16]. Similarly, the HR-TEM of both pure and doped La_2O_3 materials, did not show significant differences in the interference fringe spacing (we observed interplanar distance of *ca.* 0.310, which corresponds to the (0 0 2) plane of La_2O_3 [17]). Thus, although minor changes could be observed between the pure and doped oxides in the XRD patters, those differences are negligible by HR-TEM. Moreover, no differences in morphology were observed (by HR-TEM) between the materials prepared from PS-*co*-4-PVP or chitosan. The SAED patterns for both pure and Eu-doped oxides (see HR-TEM and SAED pattern of doped La_2O_3 prepared from chitosan

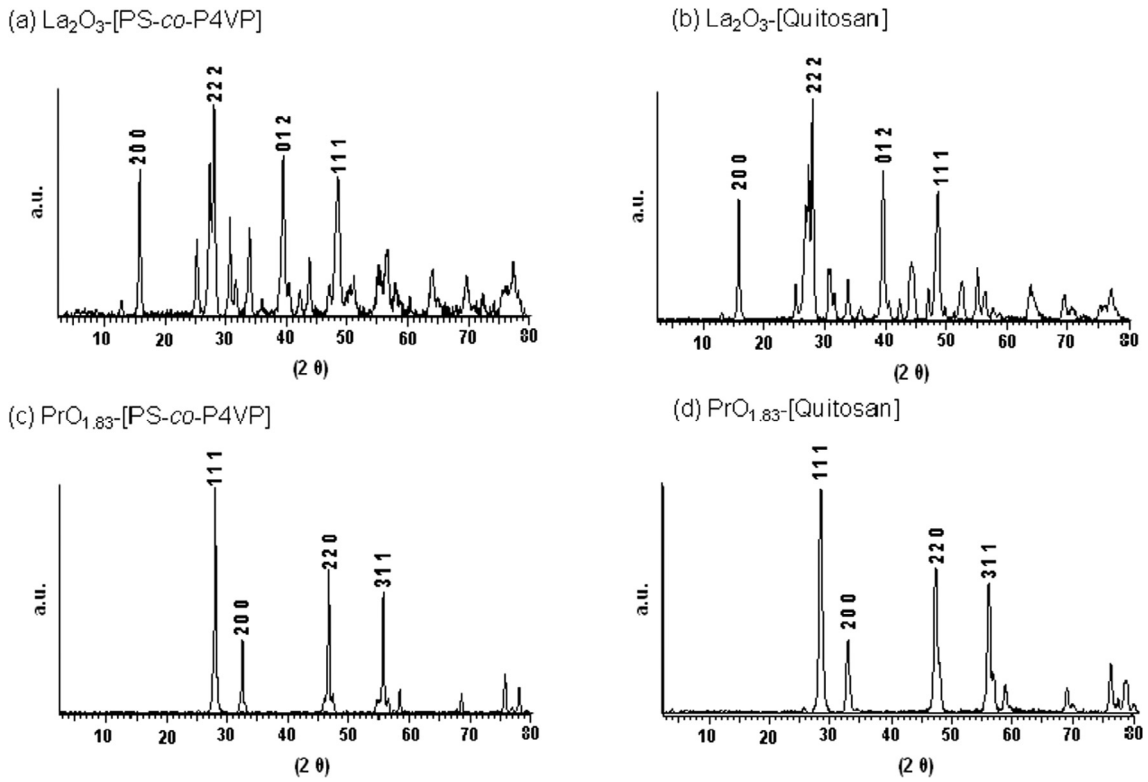

Fig. 1. XRD patterns of pure La_2O_3 and $PrO_{1,83}$ obtained from the pyrolysis of the corresponding PS-*co*-P4VP and Quitosan polymeric templates (note that, for clarity, only the more intense peaks of each phase were indexed. Not indexed peaks were also assigned to the pure phases of La_2O_3 and $PrO_{1,83}$ and not to impurities).

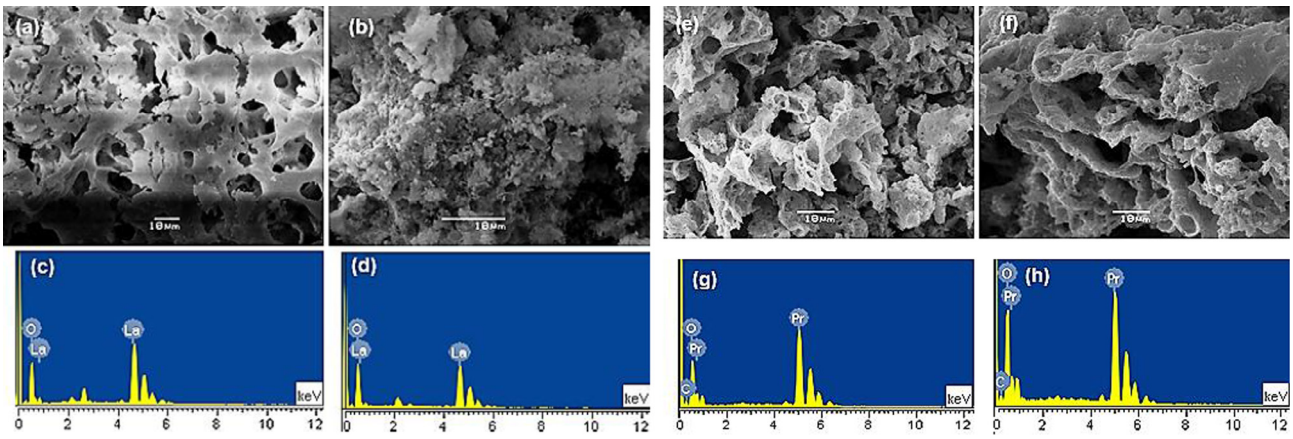

Fig. 2. SEM (up) and EDX (down) of pure La_2O_3: (a,c) from PS-*co*-P4VP. (b,d) from Chitosan. SEM (up) and EDX (down) of doped La_2O_3: (e,g) from PS-*co*-P4VP. (f,h) from Chitosan.

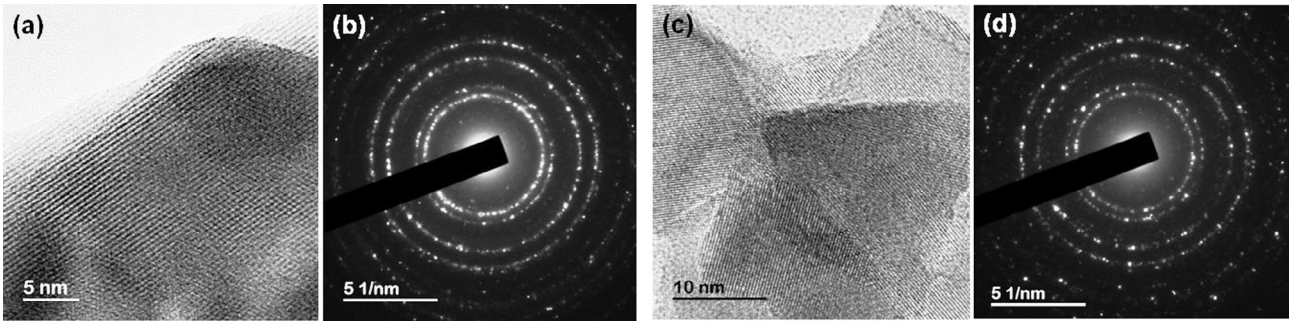

Fig. 3. HR-TEM and SAED patterns of pure $PrO_{1.83}$ obtained from PS-*co*-P4VP (a,b) and Chitosan (c,d).

in Fig. S4 in the Sup. Info), showed a high degree of crystallinity and well-defined crystallographic planes corresponding to the BCC and FCC lattices, that were previously observed by XRD for both systems.

The concentration of Eu^{+3} in the as-prepared La_2O_3 and $PrO_{1.83}$ materials was measured by ICP-mass spectroscopy, revealing higher Eu^{+3} contents in materials prepared from chitosan (0.18% Eu in doped La_2O_3 and 0.23% Eu in doped $PrO_{1.83}$) than in those of PS-*co*-4-PVP (0.1% Eu in doped La_2O_3 and 0.03% Eu in doped $PrO_{1.83}$). This lower Eu content explains the similarity of the XRD patterns of pure and doped materials when those were prepared from the PS-*co*-4-PVP template, evidencing the higher capacity of the chitosan (having $-NH_2$ and –OH groups in the repeat unit) to create macromolecular complexes.

Fig. 4 shows the emission spectra of doped La_2O_3 and $PrO_{1.83}$ prepared from both Chitosan (i.e. with higher Eu^{+3} content) and PS-*co*-P4VP. The characteristic europium $^5D_0 \rightarrow {}^7F_n$ transitions were clearly seen in all doped-oxides. Importantly, due to the nanostructured nature of the as-prepared oxides as well as the matrix effect (i.e. PS-*co*-P4VP or chitosan), a clear increasing of the luminescence intensity was observed for the doped oxides prepared from PS-*co*-P4VP. Importantly, the increasing of the emission intensity related to the $^5D_0 \rightarrow {}^7F_2$ transition of the doped $PrO_{1.83}$ prepared from PS-*co*-P4VP, was not observed when chitosan was used as a solid template. This observation can be explained by changes in both the surface effect and particle size, which indeed are affected by different polymer solid template employed in their synthesis [18,19]. Additionally, the observed red shifting of the

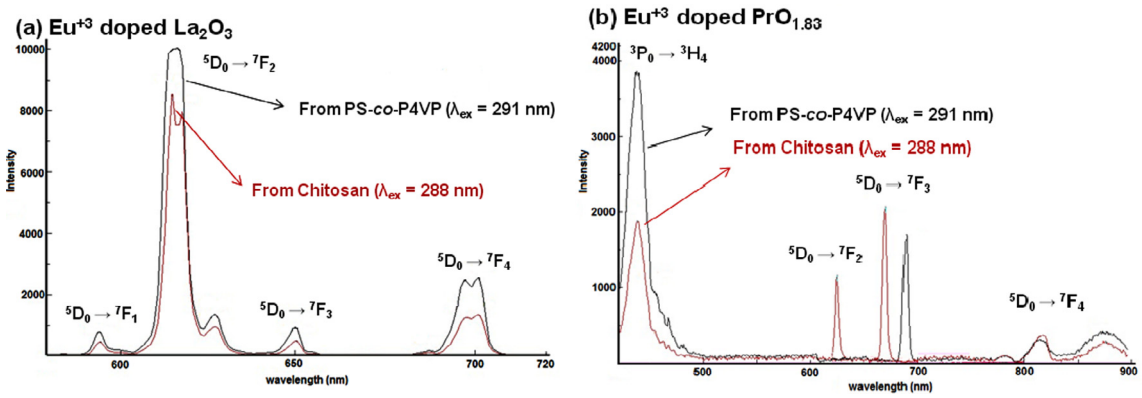

Fig. 4. Emission spectra of Eu+3 doped La_2O_3 (a) and $PrO_{1.83}$ (b) materials, obtained from Chitosan and PS-*co*-P4VP.

emission for the $PrO_{1,83}//Eu_2O_3$ with respect to those of $La_2O_3//Eu_2O_3$, can be due to the charge transfer character of the emission in this as-prepared $PrO_{1,83}//Eu_2O_3$ material [19].

4. Conclusions

In summary, pure and Eu-doped La_2O_3 and $PrO_{1,83}$ have been successfully synthesized by the pyrolysis of the precursors Chitosan·[$M(NO_3)_3//M'(NO_3)_3$] and PS-*co*-P4VP·[$M(NO_3)_3//M'(NO_3)_3$] at 800 °C. The Eu^{3+} emissions originated from the $^5D_0 \rightarrow {}^7F_n$ (n = 1, 2, 3, 4) transitions show a dependence on the nature of the polymeric solid template used in the synthesis. Thus, a higher emission intensity was observed using PS-*co*-4-P4VP as a polymeric precursor. Using PS-*co*-P4VP, the average particle size of the as prepared materials is of 25 nm, obtaining higher degree of crystallinity than those prepared from chitosan. This synthetic methodology can be used as a general pathway to prepare nanostructured doped lanthanide oxide materials that can be easily incorporated to a solid matrix to give solid state devices with potential applications in lasers and amplifiers [4].

Acknowledgements

This present work was supported by Fondecyt Project 1160241. A.P.S. is grateful to FICYT (SV-PA-13-ECOEMP-83, FC-15-GRUPIN14-106), Universidad de Oviedo (UNOV-13-EMERG-GIJON-08) and MINECO (CTQ2014-56345-P) for the funding. A.P.S. is also grateful to the COST (http://www.sips-cost.org/home/index.html), and the Juan de la Cierva and Ramón y Cajal programs.

Appendix A. Supplementary data

Supplementary data associated with this article can be found, in the online version, at http://dx.doi.org/10.1016/j.matlet.2017.07.112.

References

[1] C.N.R. Rao, A. Müller, A. K. Cheetham. Nanomaterials – an introduction, in: The Chemistry of Nanomaterials: Synthesis, Properties and Applications, C.N.R. Rao, A. Müller, A.K. Cheetham (Eds.), Wiley-VCH Verlag GmbH & Co. KGaA, Weinheim, FRG. doi: 10.1002/352760247X.ch1, 2004.

[2] T. Tan, Rare Earth Nanotechnology, 1a. ed., Pan Stanford Publishing, Singapore, 2012.

[3] K. Binnemans, Lanthanide-based luminescent hybrid materials, Chem. Rev. 109 (2012) 4283–4374.

[4] B.M. Tissue, Synthesis and luminescence of lanthanide ions in nanoscale insulating hosts, Chem. Mater. 10 (1998) 2837–2845.

[5] Zh.G. Yan, Ch.-H. Yan, Controlled synthesis of rare earth nanostructures, J. Mater. Chem. 18 (2008) 5046–5059.

[6] M.P. Pileni, Self-assembly of inorganic nanocrystals: fabrication and collective intrinsic properties, Acc. Chem. Res. 40 (2007) 685–693.

[7] M.P. Pileni, 2D superlattices and 3D supracrystals of metal nanocrystals: a new scientific adventure, J. Mater. Chem. 21 (2011) 16748–16758.

[8] Y.F. Wan, N. Goubet, P.A. Albouy, M.P. Pileni, Hierarchy in Au nanocrystal ordering in supracrystals: a potential approach to detect new physical properties, Langmuir 29 (2013) 7456–7463.

[9] C. Díaz, M.L. Valenzuela, Metallic nanostructures using oligo and polyphosphazenes as template or stabilizer in solid state, in: Encyclopedia of Nanoscience and Nanotechnology, H.S Nalwa (Ed.), American Scientific Publishers, 16, 2010, pp. 239–256.

[10] G.A.M. Hussein, Rare earth metal oxides: formation, characterization and catalytic activity thermoanalytical and applied pyrolysis review, J. Anal. Appl. Pyrolysis 37 (1996) 111–149.

[11] S. Li, H. Song, H. Yu, S. Lu, X. Bai, G. Pan, Y. Lei, L. Fan, T. Wang, Influence of annealing temperature on photoluminescence characteristics of Gd_2O_3: Eu/AAO nanowires, J. Lumin. 122–123 (2007) 876–878.

[12] R. Li, S. Gai, L. Wang, J. Wang, P. Yang, Facile synthesis and multicolor luminescent properties of uniform Lu_2O_3: Ln (Ln=Eu^{3+}, Tb^{3+}, Yb^{3+}/Er^{3+}, Yb^{3+}/Tm^{3+}, and Yb^{3+}/Ho^{3+}) nanospheres, J. Colloid Interface Sci. 368 (2012) 165–171.

[13] R. Bazzi, M.A. Flores, C. Louis, K. Lebbou, W. Zhang, C. Dujardin, S. Roux, B. Mercier, G. Leoux, E. Bernstein, P. Perriat, O. Tillement, Synthesis and properties of europium-based phosphors on the nanometer scale: Eu_2O_3, Gd_2O_3: Eu, and Y_2O_3:Eu, J. Colloid Interface Sci. 273 (2004) 191–197.

[14] C. Diaz, L. Barrientos, D. Carrillo, J. Valdebenito, M.L. Valenzuela, P. Allende, H. Geaneye, C. O'Dwyer, Solvent-less method for efficient photocatalytic α-Fe_2O_3 nanoparticles using macromolecular polymeric precursors, New J. Chem. 40 (2016) 6769–6776.

[15] C. Diaz, S. Platoni, A. Molina, M.L. Valenzuela, H. Geaney, C. O'Dwyer, Novel solid-state route to nanostructured tin, zinc and cerium oxides as potencial materials for sensors, J. Nanosci. Nanotech. 14 (2014) 7648.

[16] P.X. Huang, F. Wu, B.L. Zhu, G.R. Li, Y.L. Wang, X.P. Gao, H.Y. Zhu, T.Y. Yan, W.P. Huang, S.M. Zhang, D.Y. Song, Praseodymium hydroxide and oxide nanorods and Au/Pr_6O_{11} nanorod catalysts for CO oxidation, J. Phys. Chem. B 110 (2006) 1614–1620.

[17] G. Li, C. Peng, C. Zhang, Z. Xu, M. Shang, D. Yang, X. Kang, W. Wang, C. Li, Z. Cheng, J. Lin, Eu^{3+}/Tb^{3+}-doped $La_2O_2CO_3$/La_2O_3 nano/microcrystals with multiform morphologies: facile synthesis, growth mechanism, and luminescence properties, Inorg. Chem. 49 (2010) 10522–10535.

[18] W.W. Zhang, W.P. Zhang, P.B. Xie, M. Yin, H.T. Chen, L. Jing, Y. Zhang, L.R. Lou, Sh. Xia, Optical Properties of nanocrystalline Y_2O_3: Eu depending on ots odd structure, J. Colloid Interface Sci. Sci. 262 (2003) 588–593.

[19] P.K. Sharma, M.H. Jilavi, R. Mass, H. Schmidt, Tailoring the particles size from μm→nm scale by using a surface modifier and their size effect on the fluorescence properties of europium doped yttria, J. Lumin. 82 (1999) 187–193.